Journal of Polymer Research (2018) 25: 178
https://doi.org/10.1007/s10965-018-1572-9

ORIGINAL PAPER

Novel polySchiff base containing naphthyl: synthesis, characterization, optical properties and surface morphology

Adem Korkmaz[1] · Adnan Cetin[2] · Esin Kaya[2] · Erman Erdoğan[3]

Received: 11 May 2018 / Accepted: 9 July 2018 / Published online: 20 July 2018

Abstract

In the present work, a Schiff base was obtained from reaction of 1-naphthylamine with salicylaldehyde and its polymer (poly(NIMP)) was synthesized via oxidative polycondensation. The characterizations of the synthesized Schiff base and poly(NIMP) were determined by ^{1}H NMR, ^{13}C NMR, FT-IR, GPC and TGA techniques. The film of synthesized poly(NIMP) was prepared. The film thickness was found to be 106 μm. The optical band gap (E_g) values of the film were determined by UV-vis spectroscopy. Direct, indirect and forbidden indirect band gap (E_{gd}, E_{gid} and E_{gfid}) values of the film were found as 1.698, 1.223 and 1.461 eV, respectively. Surface properties of the film were investigated by Atomic force microscope (AFM). In the AFM results, the average surface roughness and average square root roughness were obtained as 2.46 and 3.79 nm, respectively. A negative skewness value exhibited dominant valleys while the high kurtosis value exhibited spiky features.

Keywords PolySchiff base · Conjugated polymer · Thermal properties · Optical band gap · Surface properties

Introduction

PolySchiff bases (PSs) are known as polyazomethines or polyimines. PSs including imine (-N=CH) group have superior properties due to ability of forming coordination complexes and good thermal stability [1]. PSs and their complexes are used in many applications such as photonics, optoelectronics, electronics and biological ones as well as in the various fields like hydrometallurgy, polymeric drug grafts, waste water treatment, organic synthesis and nuclear chemistry [2–6]. The conjugated PSs have also particular importance in this group. The conjugated PSs have high thermal conductivity in terms of the conjugation of these molecules and numerous aromatic heterocyclic rings. The conjugated PSs and their derivatives are used as potential brightness modifiers in ferromagnetic materials, conductors, new composites and photoelectronic materials in magnetic resonance imaging [7–9]. Besides, conjugated polymers (CPs) and their films have many advantages for potential applications such as photovoltaic cells, sensors solar cells and transistors. [10–15].

The determination of optical parameter such as optical band gap is rather significant for optic application area [16]. Also, the polymers with low band gap are desired materials for optoelectronic, photovoltaic and solar cell applications because of their processability, higher intrinsic conductivity, active surface facility, low weight, external power conversion efficiency and low-cost performance. The attention to organic photovoltaic devices build upon polymers was also importantly increased by the reported improvements in their power conversion efficiencies [17, 18].

Recently the AFM technique has been widely used for the imaging of the polymer materials. This technique allows the characterizations of surfaces at resolutions. Surface morphology has a significant effect on optical properties such as transmittance and the energy band gap [19].

In this context, we synthesized Schiff base monomer containing naphthyl and its novel conjugated polymer was obtained

Electronic supplementary material The online version of this article (https://doi.org/10.1007/s10965-018-1572-9) contains supplementary material, which is available to authorized users.

✉ Esin Kaya
esin_kaya_@hotmail.com

[1] School of Health Sciences, Muş Alparslan University, Muş, Turkey

[2] Faculty of Education, Department of Sciences, Muş Alparslan University, Muş, Turkey

[3] Faculty of Art and Sciences, Department of Physics, Muş Alparslan University, Muş, Turkey

Scheme 1 Synthesis of Schiff base monomer

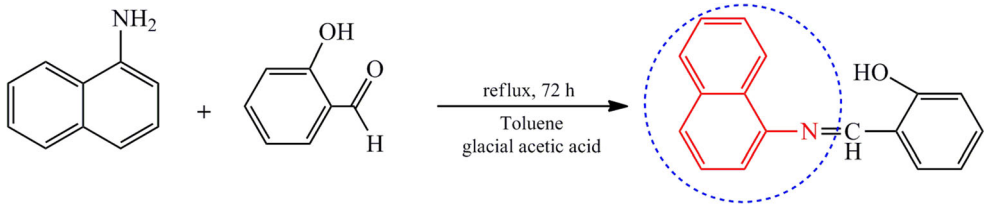

via oxidative polycondensation reaction which have further advantageous such as low cost, easy preparation and being environmentally friendly compared with other methods [20]. The synthesized Schiff base monomer and poly(NIMP) were characterized by spectroscopic analysis. The obtained poly(NIMP) had high molecular weight and long conjugated structure due to numerous repeating naphthyl groups. The film of the poly(NIMP) was prepared to examine the optical properties and surface morphology. The optical band gap of film was determined via UV-vis spectroscopy. The surface morphology of the poly(NIMP) film was analyzed by AFM.

Experiment

Materials and equipment

1-naphthylamine and salicylaldehyde were purchased as chemical reactive from Sigma Aldrich. Dimethylformamide, hydrochloric acid (HCl), sodium hypochlorite (NaOCl 10%), ethanol, potassium hydroxide (KOH) were also supplied as solvents from Merck (Darmstadt, Germany). These materials were used without purification. The infrared spectra were obtained by a Perkin Elmer Precisely Spectrum one spectrometer using an ATR head in the range of 4.000–600 cm^{-1}. Molecular weight and PDI of poly(NIMP) were determined by gel permeation chromatography (GPC) using Agilent 1100 Series, equipped with refractive index detector. UV-vis spectra were recorded by Shimadzu model UV-1800 Spectrophotometer in the wavelength between 1100 and 190 nm at room temperature. TGA measurement was performed using Perkin Elmer Pyris 1 in the range of 20–900 °C with heating rate of 10 °C min^{-1} under N_2 atmosphere. ^1H (400 MHz) and ^{13}C (100 MHz) NMR spectra were recorded on a Bruker DRX-400 high performance digital FT-NMR spectrometer. AFM was used to investigate the surface properties of poly(NIMP) film as well as a measure of the homogeneity with Ambios Q-Scope AFM device.

Synthesis and characterization of Schiff base monomer

Schiff base monomer was synthesized by dean stark method (Scheme 1). 1-naphthylamine was placed in 100 ml reaction vessel with dean-stark apparatus and dissolved in 30 ml toluene. The temperature was raised to 110 °C and one drop of glacial acetic acid was added in reaction tube. Then salicylaldehyde (1.2 mmol) was added and the color suddenly turned into orange. The solution was refluxed for 72 h. Precipitated solid was observed as the reaction continued and the occurred solid was filtrated. The solid was removed from impurities by washing with hexane and the residue was allowed at room temperature 1 day (Yield:41%, Color: light yellow). IR (ν, cm^{-1}): 3046 (aromatic C-H), 1616 (CH=N), 1589, 1569 (aromatic C=C), 1433 (-C=C-N), 1275 (C-O), 772, 750 (naphthalene rings); ^1H NMR (400 MHz, DMSO-d_6) δ (ppm): 13.48 (s, 1H, OH), 8.70 (s, 1H, -N=CH), 8.33–7.01 (m, 11H, Ar-C-H); ^{13}C NMR (100 MHz, DMSO-d_6) δ(ppm): 163.49 (HC=N), 161.16 (C-OH), 146.22, 133.99, 133.47, 132.47, 127.97, 127.00, 126.75, 126.56, 126.00, 123.29, 119.54, 119.29, 117.35, 114.08 (C atoms on aromatic ring).

Synthesis and characterization of the poly(NIMP)

The poly(1-((naphthalen-1-ylimino) methyl) phenol) (poly(NIMP)) was synthesized from Schiff base monomer in the presence of NaOCl (10%) as the oxidative reagent at 90 °C via oxidative polycondensation reaction (Scheme 2) [20]. Schiff base monomer was placed three-necked round bottom flask fitted with funnel containing NaOCl solution (10%, 10 mmol). Schiff base monomer was dissolved in dimethylformamide (4 mL) and KOH solution (5 mmol). NaOCl was added dropwise to mixture during 10 min at 60 °C. Reaction was maintained at 90 °C for 48 h. It was cooled at room temperature. The mixture was neutralized with 10 mmol HCl (37%) solution. It was washed with hot water

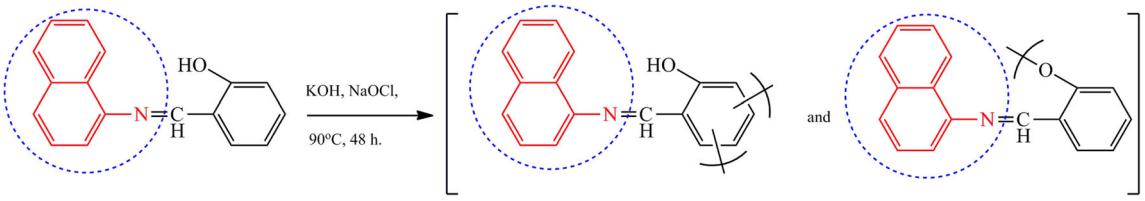

Scheme 2 Synthesis of the poly(NIMP)

(3 × 50 ml) for separating from salts. Then, poly(NIMP) was washed with ethanol to remove from impurity. Poly(NIMP) was dried in a vacuum oven at 80 °C for 24 h. (Yield: 49%. Color: dark brown). IR (ν, cm^{-1}): 3051 (aromatic C-H), 1609 (CH=N), 1592, 1570 (C=C aromatic), 1589, 1569 (aromatic C=C), 1436 (-C=C-N), 1276 (C-O), 767, 754 (naphthalene ring); ^{1}H NMR (400 MHz, DMSO-d_6) δ (ppm): 10.18 (br, 1H, OH) 9.20 (s, 1H, -N=CH), 8.16–7.31 (m, 11H, Ar-CH); ^{13}C NMR (100 MHz, DMSO-d_6) δ(ppm): 160.18 (HC=N), 157.72 (C-OH), 143.54,133.99, 129.18, 128.35, 128.26, 127.21, 126.87, 126.25, 125.94, 125.72, 124.64, 124.07, 122.81, 122.46, 115.77, 115.88, 107.82 (C atoms on aromatic ring).

Preparation of the poly(NIMP) film

The poly(NIMP) was added to 1 ml DMF until the solubilized. The solution of poly(NIMP) was stirred at room temperature for 1 h. The insoluble poly(NIMP) was removed with filter paper. The glass surface was cleaned with a piranha solution (sulfuric acid and hydrogen peroxide). Then, it was rinse with water. Later, the solution of poly(NIMP) was added dropwise to coat the film on the glass and it was left to dry automatically. The film thickness was measured as 106 µm with the micrometer (sensitivity is 0.001 mm) shown in the Fig. 1.

Results and discussion

Synthesis and characterization

PSs have attracted attention due to their ability to form coordination complexes and nonlinear optical semi-conductivity and optical, electrochemical properties [21, 22]. Therefore, initially Schiff base monomer was synthesized from reaction salicylaldehyde and 1-naphthylamine using a 1:1 M ratio via dean stark method as seen in Scheme 1. To obtain poly(NIMP), oxidative polymerization reaction of Schiff base monomer was performed using NaOCl as oxidant and air in

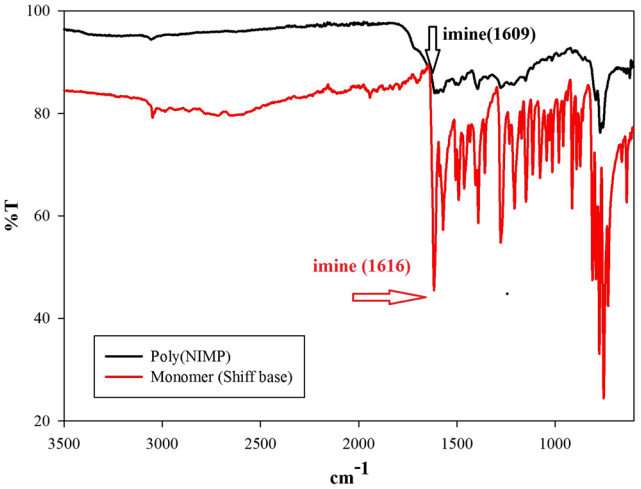

Fig. 2 FT-IR spectra of Schiff base monomer and poly(NIMP)

KOH solution at 90 °C. Although, the poly(NIMP) was insoluble in apolar solvent such as hexane and heptane, it was soluble in polar organic solvents such as dimethyl sulfoxide, tetrahydrofuran, toluene, *N*, *N*-dimethylformamide. FT-IR spectra of Schiff base monomer and poly(NIMP) were presented in Fig. 2. The imine stretching frequency at 1616 cm^{-1} supported the formation of the monomer. When compared to FT-IR spectra of Schiff base monomer and poly(NIMP), the bands of the poly(NIMP) are broader than those of the Schiff base monomer due to the repeating units and conjugated structures. The imine stretching of poly(NIMP), unlike Schiff base monomers, shifted from 1616 to 1609 cm^{-1}. These results were attributed to the formation of the poly(NIMP) [23].

^{1}H NMR and ^{13}C NMR spectra of Schiff base monomer and poly(NIMP) were also recorded in deuterated DMSO. When ^{1}H NMR spectra were examined, the hydroxyl and imine protons of the Schiff base monomer were seen at 13.48 and 8.70 ppm, respectively. The hydroxyl and imine protons of poly(NIMP) were observed at 10.18 and 9.20 ppm, respectively. Furthermore, aromatic protons were observed in the range 8.16–7.31 ppm for poly(NIMP) and 8.33–7.01 ppm for Shiff base monomer. The broad and

Fig. 1 Images of 106 µm coated poly(NIMP) film and micrometer

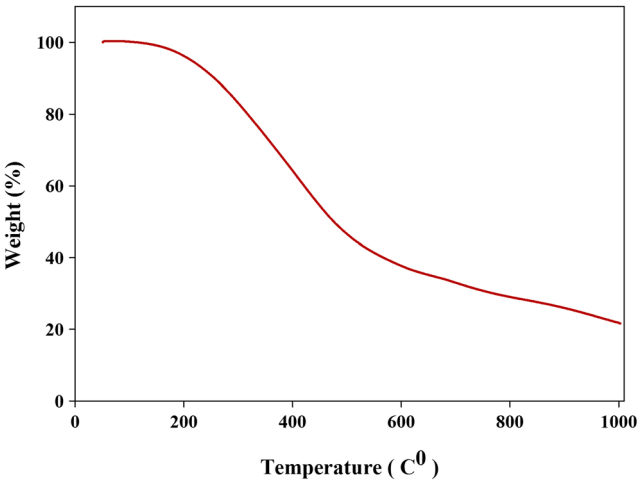

Fig. 3 TGA curve of the poly(NIMP)

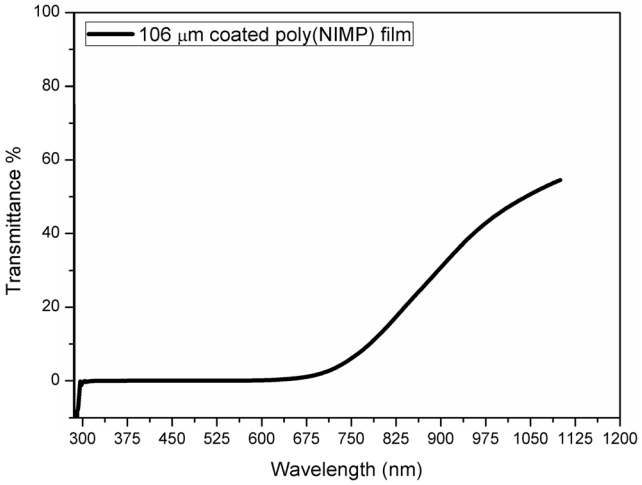

Fig. 4 The graph of transmittance versus wavelength for the poly(NIMP) film

shifted peaks also proved the formation of poly(NIMP) [23]. When ^{13}C NMR spectra were examined the hydroxyl and imine carbon peaks of Schiff base monomer and poly(NIMP) were observed at 161.16, 157.72 and 163.49, 160.18 ppm, respectively. The hydroxyl and the imine carbon peaks of poly(NIMP) shifted approximately 4 ppm to lower frequency. Moreover, aromatic carbon peaks were observed in the range 115.69 to 155.81 ppm and coupling carbon (-C-C) peaks were observed in the synthesized poly(NIMP) structure at 129.18 and 107.82 ppm.

The number molecular weight and PDI of the poly(NIMP) were determined by GPC. *Mn* and *Mw* values were calculated as 3.52×10^5 and 3.65×10^5, respectively. PDI value was determined as 1.04, too. A novel polymer with high molecular weight was obtained. Thermal degradation behavior of the poly(NIMP) was investigated by thermogravimetric analysis (TGA). This process was carried out in the temperature range 25–1000 °C with a heating rate of 10 °C / min under nitrogen atmosphere. TGA thermogram was presented in Fig. 3. The results were also summarized in Table 1. The weight losses % at 400, 600, 800 and 1000 °C of poly(NIMP) were found as 35, 62, 72 and 78, respectively. The results showed that the poly(NIMP) had high residue due to the long-conjugated band systems [23]. The poly(NIMP) exhibited a linear decline up to 500 °C, after which the rate of weight loss significantly reduced.

Optical properties

UV-Vis spectroscopy measurements are commonly used for investigating optical properties [24]. PSs having aromatic structures such as naphthyl group have drawn attention due to their unique optical properties. In addition, aromatic π-conjugated naphthyl structures are important materials due to π–π intermolecular interactions for optical and electronical applications [25, 26]. Hence, optical properties of the prepared film containing imine and naphthyl groups were investigated in the present work. Transmittance (T) and absorbance (A) values of the poly(NIMP) film were recorded to investigate optical properties as a function of the wavelength.

The transmittance graph for the poly(NIMP) film was shown in Fig. 4. The transmittance value of the poly(NIMP) film increased almost constantly with very small increments in the range 300–675 nm. After 675 nm, the transmittance value was clearly increased and reached maximum at 1100 nm. It was maximum at 55%. While the average transmittance value of the poly(NIMP) film was determined to be 31.74% between 190 and 1100 nm, it was calculated as 1.24% in the visible region. The transparency feature of the poly(NIMP) film was almost nonexistent.

A graph of absorbance versus wavelength was plotted for the poly(NIMP) film in Fig. 5. It was observed that the poly(NIMP) film started absorbing at 1100 nm due to

Table 1 Thermogravimetric analysis data of the poly(NIMP)

	[a]T_i(°C)	Weight loss % at 400 °C	Weight loss % at 500 °C	Weight loss % at 600 °C	Weight loss % at 700 °C	Weight loss % at 800 °C	Weight loss % at 1000 °C
Poly(NIMP)	150	35	53	62	67	72	78

[a] *Initial decomposition temperature*

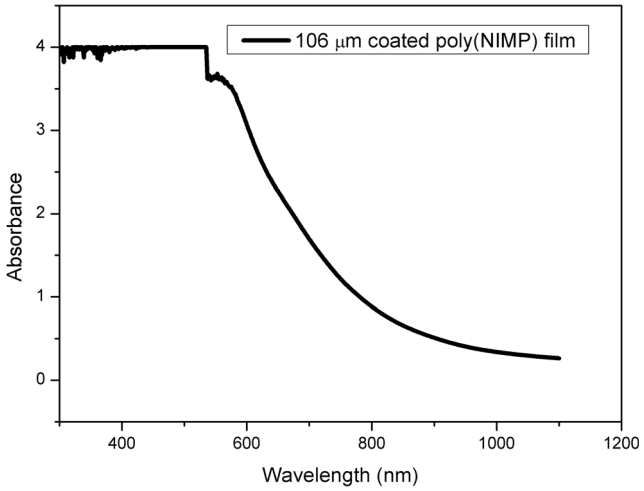

Fig. 5 The graph of absorbance versus wavelength for the poly(NIMP) film

conjugation contribution of the numerous repeating naphthyl units. It is well known that the extension of conjugation degree leads to red-shift in the absorption spectra [27]. The poly(NIMP) film showed a sharp increase in the absorption graph between 600 and 800 nm. Then there was a slight decrease and a steep increase. Ultimately, the absorption remained constant in the range of 285–580 nm. While the absorption bands at shorter wavelengths (285–600 nm) were related to n-π* and π-π* electronic transitions of the imine, phenolic OH and naphthyl groups in poly(NIMP) film structure, the absorption bands at longer wavelengths (600–800 nm) were related to charge transfer of conjugated units [28–30]. Various strategies have been used in designing new photovoltaic polymers such as broadening the absorption band [31, 32], enhancing the charge carrier mobility with conjugated bridges [33] and producing lower bandgap polymers as a result of which the absorption of the conjugated polymers is red-shifted [34, 35].

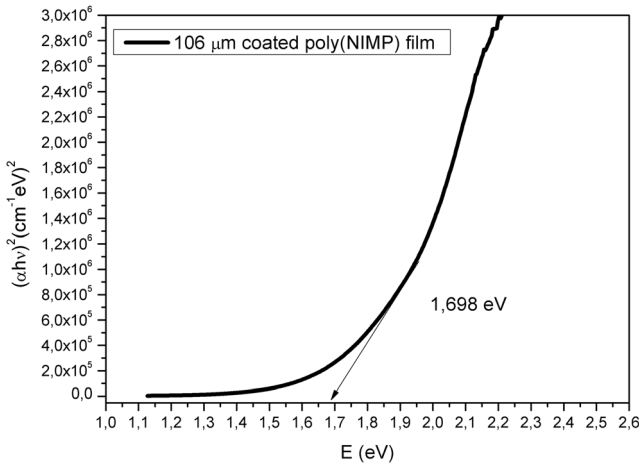

Fig. 6 The graph of $(\alpha h\nu)^2$ versus photon energy for the poly(NIMP) film

Table 2 E_g values of the poly(NIMP) film

Thickness	E_{gd}	E_{gid}	E_{gfid}
106 (μm)	1.698 (eV)	1.223 (eV)	1.461 (eV)

To find E_{gd} of the poly(NIMP) film, the photon energy versus $(\alpha h\nu)^2$ was plotted by using Tauc equation (Fig. 6) [36].

As shown in Fig. 6, the E_{gd} value of the poly(NIMP) film was found to be 1.698 eV. To find the value of the E_{gid}, the photon energy versus $(\alpha h\nu)^{1/2}$ was plotted (Fig. 7). E_{gid} value of the poly(NIMP) film was found to be 1.223 eV. The E_{gid} value was lower than the E_{gd} value (see Table 2). It was also seen that the direct transition was sharper than the indirect one (Fig. 6 and Fig. 7). In this case, it can be said that direct transition is more appropriate than the indirect ones. Direct band gap refers to the case that the highest valence band and the lowest conduction band has the same moment; hence electrons can direct jump from valence to conduction. Then for indirect, there is a momentum difference and some other factors must come in to balance the difference (phonons perhaps). Direct band gap transition will cause solar energy to be absorbed more efficiently and hence better photovoltaic devices.

A graph of E (eV) vs $(\alpha h\nu)^{1/3}$ was plotted for the poly(NIMP) film in Fig. 8. The E_{gfid} for the poly(NIMP) film was found as 1.461 eV.

The poly(NIMP) had low E_g values. The low-band gap polymers which have a band gap smaller than 1.6 eV are particularly attractive in organic photovoltaics (OPV), photodetectors (PDs), and ambipolar field-effect transistors (FETs) [14, 27, 37]. In many

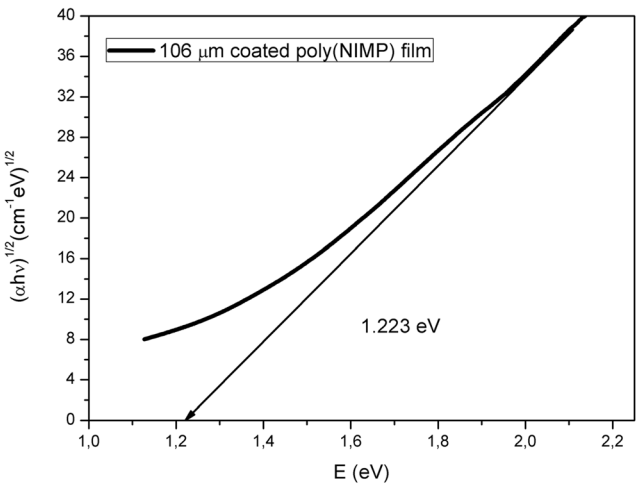

Fig. 7 The graph of $(\alpha h\nu)^{1/2}$ versus photon energy for the poly(NIMP) film

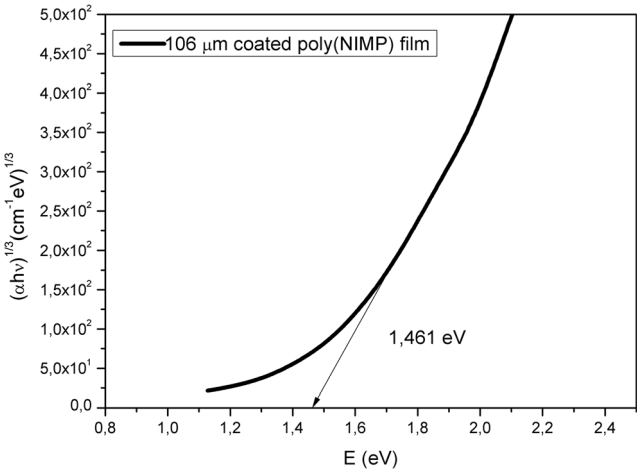

Fig. 8 The graph of $(\alpha h\nu)^{1/3}$ versus photon energy for the poly(NIMP) film

researches, the E_g values of the conjugated polymers in photovoltaic applications were found between 1.6 and 2.5 eV [38–41]. Furthermore, Niu et al. synthesized two novel functional conjugated polySchiff bases with triphenylamine unit having conjugation throughout the molecule chain by condensation polymerization of 4,4′-biamine triphenylamine and dialdehydes in solution. They calculated approximately the optical band gaps values as 2.33 and 2.19 eV for the obtained polymers. One of the polymers was used as the polymer electroluminescence (EL) device [42]. Kaya et al. synthesized the poly(phenoxy-imine) anchored with the carboxyl group exhibiting photovoltaic cell property [43]. Recently, a conjugated polySchiff base having low band gap with thieno[3,2-b] thiophene and 1,2,4-triazole groups was reported by our group [44]. The poly(NIMP) with low band gap obtained without doping and complex formation makes this work valuable for many industrial applications.

Surface morphology

AFM was used to examine the morphology and surface texture of the poly(NIMP) film. The two (2D)- and three-dimensional (3D) images of the film were presented in Fig. 9. In the AFM images, black areas appeared in a few places, but yellow areas appeared in more places. While the black regions represented the valley in the surface, the white regions represented the peaks. As shown in Fig. 9, the distance between the lowest and highest point in the scanned area was 30 nm.

In the AFM surface analysis, the average surface roughness giving the height deviation was found to be 2.46 nm. The average square root roughness which represented the standard deviation of the surface heights was found to be 3.79 nm. The total roughness which was the sum of the maximum height and depth for the entire measurement length was 42.57 nm on the 2D-AFM graph in Fig. 9. The skewness value that was a measure of asymmetry of surface deviations was −1.66. Obtaining as a negative skewness value means that the valleys on the film surface were more dominant than the peaks. The kurtosis value; the measure of the sharpness of the height distributions, was 12.36. A kurtosis value larger than 3 indicates high peaks and low valleys with a spiky surface. Excessive positive kurtosis is called leptokurtic distribution meaning high peak [45].

The histogram analysis and line profile for vertical cross-section of the film in 9 μm × 9 μm scan area were shown in Fig. 10 (a) and (b). The histogram was a plot of adjacent peaks. Each peak symbolized a height sequence. The cross-section plot of the film had many thorny faces for red line region. The height of the largest peak of the film was about 7.7 nm [46].

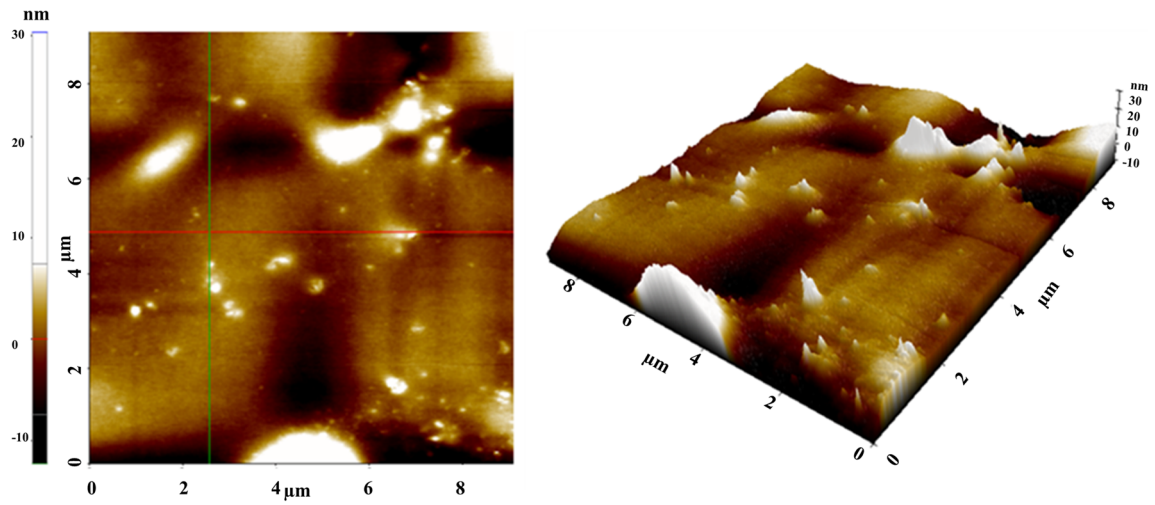

Fig. 9 2D and 3D AFM images of produced poly(NIMP) film

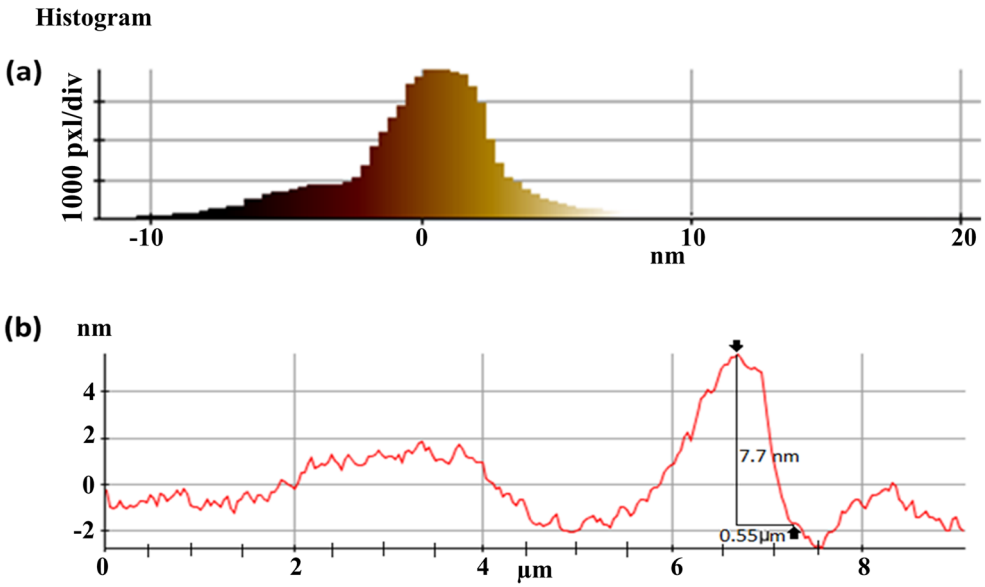

Fig. 10 **a** The histogram analysis and (**b**) Cross section for plots of the poly(NIMP) film

As seen in Fig. 11, the height distribution graph was attained using the AFM tool. It was associated with the symmetric distribution on the surfaces. Compared to the normal, it has a stronger peak, more rapid decay, and heavier tails due to the high value of kurtosis. Furthermore, Gauss curve of the height distribution graph of poly(NIMP) film shows homogeneous grain distribution.

Conclusions

A novel conjugated polySchiff base was synthesized and characterized. The optical properties of prepared polySchiff base film were examined. Direct, indirect and forbidden indirect band gap values of the poly(NIMP) film were found as 1.698, 1.223 and 1.461 eV, respectively. The low E_g values for poly(NIMP) film were obtained due to high polymer degree and conjugation. In the result of AFM, the surface of film had low roughness values. The skewness value of the poly(NIMP) film was obtained as negative which peaks to a predominance of valleys. The kurtosis value was greater than 3 for the poly(NIMP) film. The novel polySchiff base film having low optical band gap and good surface morphology might be a good candidate for optoelectronic and photovoltaic devices.

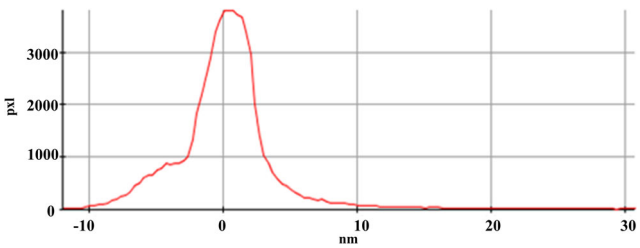

Fig. 11 Gauss curve of the height distribution graph of poly(NIMP) film

References

1. Grigoras M, Catanescu CO (2004) Imine oligomers and polymers. J Macromol Sci Part C: Polym Rev 44(2):131–173
2. Dineshkumar S, Muthusamy A (2016) Synthesis and spectral characterization of cross linked rigid structured Schiff base polymers: effect of substituent position changes on optical, electrical, and thermal properties. Polym Plast Technol Eng 55(4):368–378
3. Qureshi F, Khuhawar MY, Jahangir TM, Channar AH (2016) Synthesis, characterization and biological studies of new linear thermally stable Schiff base polymers with flexible spacers. Acta Chim Slov 63(1):113–120
4. Kaliyappan T, Rajagopan S, Kannan P (2004) New polymeric Schiff base and its metal complexes. J Appl Polym Sci 91(1): 494–500
5. Zhou J, Gao F, Jiao T, Xing R, Zhang L, Zhang Q, Peng Q (2018) Selective cu (II) ion removal from wastewater via surface charged self-assembled polystyrene-Schiff base nanocomposites. Colloids Surf A Physicochem Eng Asp 545:60–67
6. Kaliyappan T, Kannan P (2000) Co-ordination polymers. Prog Polym Sci 25(3):343–370
7. Jiang L, Sun W (2005) A novel bithiazole-containing polymeric complex with soft ferromagnetism. Polym Adv Technol 16(8): 646–649
8. He B, Sun W, Wang M, Shen Z (2004) Synthesis and magnetic property of a novel SWNT-poly (Schiff base)-Nd3+ complex. Mat Chem Phys 87(1):222–226
9. Ogata N (1991) Novel synthetic methods of condensation polymers and their applications as new composite and opto-electronic materials. Pure Appl Chem 63(7):951–960
10. Zhang H, Zhang S, Gao K, Liu F, Yao H, Yang B, Hou J (2017) Low band-gap conjugated polymer based on diketopyrrolopyrrole units and its application in organic photovoltaic cells. J Mater Chem A 5(21):10416–10423
11. McQuade DT, Pullen AE, Swager TM (2000) Conjugated polymer-based chemical sensors. Chem Rev 100(7):2537–2574
12. Nikolka M, Nasrallah I, Rose B, Ravva MK, Broch K, Sadhanala A, Illig S (2017) High operational and environmental stability of high-mobility conjugated polymer field-effect transistors through the use of molecular additives. Nat Mater 16(3):356–362

13. Moliton A, Hiorns RC (2004) Review of electronic and optical properties of semiconducting π-conjugated polymers: applications in optoelectronics. Polym Int 53(10):1397–1412
14. Li G, Chang WH, Yang Y (2017) Low-band gap conjugated polymers enabling solution-processable tandem solar cells. Nat Rev Mater 2(8):1–13
15. Kaya E, Gündüz B, Çetin A (2016) Synthesis and characterization of conjugated polymers containing phenyl and bithiophene: controlling of optical properties with molarity. Colloid Polym Sci 294(2):339–345
16. Neumann H, Hörig W, Reccius E, Sobotta H, Schumann B, Kühn G (1979) Growth and optical properties of CuGaTe2 thin films. Thin Solid Films 61(1):13–22
17. Shaheen SE, Brabec CJ, Sariciftci NS, Padinger F, Fromherz T, Hummelen JC (2001) 2.5% efficient organic plastic solar cells. Appl Phys Lett 78(6):841–843
18. Xue J, Uchida S, Rand BP, Forrest SR (2004) Asymmetric tandem organic photovoltaic cells with hybrid planar-mixed molecular heterojunctions. Appl Phys Lett 85(23):5757–5759
19. Yang Z, Moffa M, Liu Y, Li H, Persano L, Camposeo A, Nam CY (2018) Electrospun conjugated polymer/fullerene hybrid fibers: photoactive blends, conductivity through tunneling-AFM, light scattering, and perspective for their use in bulk-heterojunction organic solar cells. J Phys Chem C 122(5):3058–3067
20. Mart H (2006) Oxidative polycondensation reaction. Des Monomers Polym 9(6):551–588
21. Deng F, Li X, Ding F, Niu B, Li J (2018) Pseudocapacitive energy storage in Schiff Base polymer with Salphen-type ligands. J Phys Chem C 122(10):5325–5333
22. Dineshkumar S, Muthusamy A (2017) Investigation of aggregation induced emission in 4-hydroxy-3-methoxybenzaldehyde azine and polyazine towards application in (opto) electronics: synthesis, characterization, photophysical and electrical properties. Des Monomers Polym 20(1):234–249
23. Kaya İ, Gökpınar M, Kamacı M (2017) Reaction conditions, photophysical, electrochemical, conductivity, and thermal properties of polyazomethines. Macromol Res 25(7):739–748
24. Kiymaz D, Sezgin M, Sefer E, Zafer C, Koyuncu S (2017) Carbazole based DA-π-A chromophores for dye sensitized solar cells: effect of the side alkyl chain length on device performance. Int J Hydrogen Energ 42(12):8569–8575
25. Grigoras M, Catanescu O, Colotin G (2001) Poly(Schiff)bases containing 1,10 -bisnaphthyl moieties: synthesis and characterization. Macromol Chem Phys 202(11):2262–2266
26. Miyaji T, Azuma T, Asaoka E, Nakamura S (2000) Regeneration of polycondensation of wholly aromatic poly(azomethine)s with 1,5- or 2,6-substituted naphthalene moiety in main chain. J Polym Sci Part A Polym Chem 38:1064–1072
27. Wu W, Liu Y, Zhu D (2010) π-Conjugated molecules with fused rings for organic field-effect transistors: design, synthesis and applications. Chem Soc Rev 39(5):1489–1502
28. Li Y, Zou Y (2008) Conjugated polymer photovoltaic materials with broad absorption band and high charge carrier mobility. Adv Mat 20(15):2952–2958
29. Kandulna R, Choudhary RB (2017) Robust electron transport properties of PANI/PPY/ZnO polymeric nanocomposites for OLED applications. Optik 144:40–48
30. Kim YA, Kang M, Jeon YJ, Hwang K, Kim YJ, Jang SY, Kim DY (2017) Structure–property relationship of D–A type copolymers based on phenanthrene and naphthalene units for organic electronics. J Mat Chem C 5(39):10332–10342
31. Li Z, Wang M, Li H, He J, Li N, Xu Q, Lu J (2017) Rewritable ternary data storage devices based on polymethacrylate containing pendent azobenzene–naphthalene with the combined effects of conformation change and charge traps. J Mat Chem C 5(33):8593–8598
32. Hou J, Yang C, He C, Li Y (2006) Poly [3-(5-octyl-thienylene-vinyl)-thiophene]: a side-chain conjugated polymer with very broad absorption band. Chem Comm (8):871–873
33. Zhou E, Tan ZA, Huo L, He Y, Yang C, Li Y (2006) Effect of branched conjugation structure on the optical, electrochemical, hole mobility, and photovoltaic properties of polythiophenes. J Phys Chem B 110(51):26062–26067
34. Zhou E, Tan ZA, Yang C, Li Y (2006) Linking polythiophene chains through conjugated bridges: a way to improve charge transport in polymer solar cells. Macromol Rapid Commun 27(10):793–798
35. Scharber MC, Mühlbacher D, Koppe M, Denk P, Waldauf C, Heeger AJ, Brabec CJ (2006) Design rules for donors in bulk-heterojunction solar cells—towards 10% energy-conversion efficiency. Adv Mat 18(6):789–794
36. Tauc J, Menth A (1972) States in the gap. J Non-Cryst Solids 8-10: 569–585
37. Roncali J (1997) Synthetic principles for bandgap control in linear π-conjugated systems. Chem Rev 97(1):173–206
38. Demadrille R, Firon M, Leroy J, Rannou P, Pron A (2005) Plastic solar cells based on Fluorenone-containing oligomers and Regioregular alternate copolymers. Adv Funct Mat 15(9):1547–1552
39. Wu CG, Hsieh CW, Chen DC, Chang SJ, Chen KY (2005) Low band gap-conjugated polymer derivatives. Synth Met 155(3):618–622
40. Kim IT, Elsenbaumer RL (2000) Synthesis, characterization, and electrical properties of poly (1-alkyl-2, 5-pyrrylene vinylenes): new low band gap conducting polymers. Macromol 33(17):6407–6411
41. Hou J, Chen HY, Zhang S, Chen RI, Yang Y, Wu Y, Li G (2009) Synthesis of a low band gap polymer and its application in highly efficient polymer solar cells. J Am Chem Soc 131(43):15586–15587
42. Niu HJ, Huang YD, Bai XD, Li X (2004) Novel poly-Schiff bases containing 4, 4′-diamino-triphenylamine as hole transport material for organic electronic device. Mat Lett 58(24):2979–2983
43. Kaya İ, Ayten B, Şenol D (2018) Syntheses of poly (phenoxy-imine) s anchored with carboxyl group: characterization and photovoltaic studies. Opt Mater 78:421–431
44. Cetin A, Korkmaz A, Kaya E (2018) Synthesis, characterization and optical studies of conjugated Schiff base polymer containing thieno [3, 2-b] thiophene and 1, 2, 4-triazole groups. Opt Mater 76: 75–80
45. Gizli N (2011) Morphological characterization of cellulose acetate based reverse osmosis membranesby atomic force microscopy (FM) effect of evaporation time. Chem Chem Technol 5(3):327–331
46. Yoshida W, Cohen Y (2003) Topological AFM characterization of graft polymerized silica membranes. J Membr Sci 215(1–2):249–264